

# Exchange interaction and magnetoresistance in $\text{La}_{2/3}\text{Ca}_{1/3}\text{MnO}_3$ : experiment and models

A. B. Beznosov, B. I. Belevtsev, E. L. Fertman, and V. A. Desnenko

*B. Verkin Institute for Low Temperature Physics and Engineering of the National Academy of Sciences of Ukraine, 47 Lenin Ave., Kharkov 61103, Ukraine*  
E-mail: beznosov@ilt.kharkov.ua

D. G. Naugle, K. D. D. Rathnayaka, and A. Parasiris

*Department of Physics, Texas A & M University, College Station, TX 77843, USA*

Received March 5, 2002

The magnetization  $M(T)$  and electrical resistivity  $\rho(T)$  of a  $\text{La}_{2/3}\text{Ca}_{1/3}\text{MnO}_3$  film have been studied in the temperature range  $5 \text{ K} \leq T \leq 320 \text{ K}$  in the magnetic field intervals  $10 \text{ Oe} \leq H \leq 400 \text{ Oe}$  and  $0 \leq H \leq 50 \text{ kOe}$ , respectively. It is found that the  $M(T)/M(0)$  value is larger than that predicted by the conventional molecular field model below the Curie point  $T = 267 \text{ K}$ , and that the  $\ln \rho(T)$  dependence is close to linear in the temperature range  $80 \text{ K} < T < 200 \text{ K}$  (accordingly,  $\partial \ln \rho / \partial T$  is constant in this region). A model of the electrical conductivity and magnetoresistivity of the system describing qualitatively the experimental results is proposed (the  $\Delta m \tau$  model). The model includes a thermally activated (with characteristic energy  $\Delta$ ) mechanism of conductivity, dependence of the concentration and the effective mass ( $m$ ) of the itinerant charge carriers on the magnetization, as well as scattering (with characteristic time  $\tau$ ) of the charge carriers by static breakings of the translational symmetry, thermal fluctuations of the magnetic order, and phonons.

PACS: 75.30.Vn, 72.80.Ga, **81.05.-t**

## 1. Introduction

Complex oxides containing manganese ions  $\text{Mn}^{3+}$  and  $\text{Mn}^{4+}$  have been attracting much attention in physics and technology in the last 10 years due to the «colossal magnetoresistance (CMR) effect» discovered in them: the electrical resistance of the compounds decreases substantially (in orders of magnitude) when an external magnetic field is applied to a sample in the vicinity of the Curie temperature (see reviews [1–6]). The nature of this phenomenon is being studied intensively; the main directions of the research are outlined in the above-mentioned reviews. We note here also the following original papers, references to which will be made below [7–14].

The key point in an understanding of the CMR mechanisms is elucidating of the nature of changes of the electrical resistance on passage through the

Curie point, first of all in the absence of the external magnetic field. The present work is devoted to an experimental study of the problem as well as to a theoretical modeling of the phenomenon.

The dependences of the magnetization and electrical conductivity of a  $\text{La}_{2/3}\text{Ca}_{1/3}\text{MnO}_3$  film on the temperature and magnetic field are studied experimentally and analyzed. A model of the electrical conductivity and magnetoresistive behavior is proposed ( $\Delta m \tau$  model). The model includes a thermally activated (with the characteristic energy  $\Delta$ ) mechanism of conductivity, dependence of the concentration and effective mass ( $m$ ) of the itinerant charge carriers on the magnetization, as well as scattering (with the characteristic time  $\tau$ ) of those carriers by static breakings of translational symmetry, thermal fluctuations of the magnetic order, and phonons.

## 2. The $\Delta m\tau$ model of conductivity

The proposed effective model of conductivity is based on the concept of thermal excitation of the charge carriers from localized states to itinerant states. We do not specify here the type of charge carriers, but for simplicity, without any loss in generality, we call them electrons. In this picture, above the Curie point the charge carriers are localized, so that their motion between the crystal sites can only be of the thermally activated kind. At the same time they appear to be nearly free in the ferromagnetically ordered state. Thus their activation energy has to be dependent on the magnetic order parameter.

### 2.1. Activation energy

Analysis of the results of our present measurements of the electrical resistivity and magnetization of the  $\text{La}_{2/3}\text{Ca}_{1/3}\text{MnO}_3$  film (see Secs. 5, 6) has shown that the dependence of the activation energy  $\Delta$  on the ferromagnetic order parameter of the system  $\sigma = M(T, H)/M_0$  in a vicinity of the Curie point  $T_C$  is close to linear (here  $M$  is the magnetization,  $T$  is the temperature,  $H$  is the magnetic field, and  $M_0$  is the magnetization at  $T=0$ ). On the other hand, the conductivity must be of the nonactivated kind at  $T = 0$  (the experiment gives a finite value of the corresponding electrical resistivity of the system  $\rho$ ). Thus we choose the simplest dependence  $\Delta(\sigma)$  satisfying the above mentioned requirements, in the form

$$\Delta = \Delta_0(1 - \sigma), \quad (1)$$

where  $\Delta_0$  is the activation energy in the paramagnetic region and will be determined in the model by fitting to the experimental data.

Expression (1) gives for the concentration of the electrons in the «conduction band» the value

$$n = n_0 e^{-\frac{\Delta_0(1-\sigma)}{T}}, \quad (2)$$

where  $n_0$  is the concentration of the conduction electrons in the completely ordered system ( $\sigma = 1$ ).

Note that a dependence of the form in Eq. (2) was established for the concentration of the conduction electrons of  $\text{EuO}$  in Ref. 8.

### 2.2. Effective mass of charge carriers

The hopping integral of the electrons in the «conduction band» depends on the mutual orientation of the local spins of nearest magnetic ions [5], so that their effective mass  $m^*$  also depends on  $\sigma$ :

$$m^* = m_0^* \frac{2}{1 + \sigma}. \quad (3)$$

Here  $m_0^*$  is the effective mass of the perfect crystal ( $\sigma = 1$ ) and will be considered further as a fitting parameter of the model.

The expression (3) has been obtained by the averaging of the hopping integral over the crystal with a subsequent transition to the effective mass representation in a model of magnetization in which the local quantization axes for the itinerant electrons (i.e., the directions of the local magnetic moments considered as classical vectors) are deflected from the easy magnetization axis by the same polar angle at every Mn site, and the azimuth angles are randomly distributed uniformly in the interval  $(0, 2\pi)$ .

### 2.3. Transport relaxation time

The electrical resistivity of the system is calculated in the model by the Drude formula

$$\rho = \frac{m^*}{e^2 n \tau}, \quad (4)$$

where  $e$  is the electron charge,  $m^*$  and  $n$  are determined by Eqs. (1)–(3), and the transport relaxation time  $\tau$  is defined by the sum

$$\tau^{-1} = \tau_{st}^{-1} + \tau_{ph}^{-1} + \tau_m^{-1}. \quad (5)$$

Here  $\tau_{st}$ ,  $\tau_{ph}$  and  $\tau_m$  are the characteristic times for the scattering by the static breakings of the translational symmetry of the system (this is principally because of the random distribution of the La and Ca ions in the crystal), phonons, and fluctuations of the local magnetic moments, respectively.

Taking into account Eqs. (1), (2), (4), and (5), and using the theoretical approaches from Refs. 15–17, we write the expression for the electrical resistivity of the system in the form

$$\rho = e^{\frac{2}{3}} \frac{\Delta}{T} (\rho_{st} + \rho_{ph} + \rho_m). \quad (6)$$

Here the resistivity  $\rho_{st}$ , caused by the static breakings of the crystal-lattice translational symmetry, is given by

$$\rho_{st}(\sigma) = \rho_0 \left( \frac{2}{1 + \sigma} \right)^2, \quad (7)$$

where Eq. (3) and the theory of Ref. 15 have been taken into account.

The resistivity  $\rho_{ph}$ , caused by the electron–phonon scattering, is evaluated by the Bloch–Grüneisen formula [16]

$$\rho_{\text{ph}} = 4 \rho_D \left( \frac{T}{\Theta_D} \right)^5 \int_0^{\frac{\Theta_D}{T}} \frac{x^5 dx}{(e^x - 1)(1 - e^{-x})}, \quad (8)$$

where the Debye temperature  $\Theta_D$  is taken equal to 440 K (by our estimate made using the sound velocity from Ref. 18), which is in accordance with other estimates [6,19].

The resistivity  $\rho_m$  caused by the electron scattering on the disordered local spins is evaluated using the Kasuya expression [17], modified for the present case by replacing the constant effective mass by a function of magnetization [Eq. (3)]:

$$\rho_m = \rho_{m\infty} \left( \frac{2}{1 + \sigma} \right)^2 S(S - S\sigma^2 - \sigma + 1). \quad (9)$$

Note that as one can see from Eqs. (6), (7), and (9), all three scattering times in Eq. (5) have the same dependence on  $n$  ( $\tau \propto n^{-1/3}$ ),  $\tau_{\text{st}}$  and  $\tau_m$  have the same dependence on  $m^*$  ( $\tau_{\text{st}(m)}^{-1} \propto m^*$ ).

Exponential dependences of the electrical resistivity, compatible with Eq. (6) (i.e., with the argument of the exponential function being linearly dependent on magnetization), were observed experimentally in Refs. 7–9. Other forms of the  $\rho(\sigma)$  dependence were proposed in Refs. 7, 11–14. On our opinion, these last do not have as good agreement with the known experimental data (see Refs. 1–6) and with those obtained in this work.

### 3. The modified molecular field model for magnetization

The local spin  $S$  in Eq. (9) was put equal to 2, and the reduced magnetization  $\sigma = M/M_0$  was estimated in the modified molecular field model. This model differs from the conventional form (see, for example, [20]) by the additional fitting parameters  $a$  and  $h$ . They formally take into account the effect of spontaneous magnetization on the interatomic exchange parameter and the effect of the short-range order on the charge-carrier scattering above the Curie temperature. The latter is substantial in the case of a short mean free path of the carriers, because they are localized in the absence of magnetic order, as is evidenced by the change of character of the conductivity from metallic to semiconductive when going from the ferromagnetic to the paramagnetic state of the oxide.

The ferromagnetic order parameter in the model is defined by the following equation:

$$\sigma = B_S \left( \frac{h}{T} + \frac{3S}{S+1} \frac{T_C(1 + a\sigma^2)}{T} \sigma \right). \quad (10)$$

Here  $B_S(x)$  is the Brillouin function for spin  $S = 2$ ,  $T_C$  is the Curie temperature,  $h$  is a fictive magnetic field modeling the effect of short-range magnetic order above  $T_C$ , and  $a$  is a magnetoelastic parameter describing the magnetostrictive shift of  $T_C$  [21].

Note that the value  $S = 2$  for the local spin used in the model corresponds to the spin of the  $\text{Mn}^{3+}$  ion but not to the spin  $S = 3/2$  of the  $\text{Mn}^{4+}$  ion, which must actually be regarded as the local spin. This is done just because it gives a better fit (compared to  $S = 3/2$ ) of the experimental data in the low-temperature region, where molecular field theory, used in the model over the whole temperature range for simplicity, is not valid *a priori*. Thus, such a substitution can be made without any fundamental significance. In the most important region, in the vicinity of  $T_C$ , the value  $S = 3/2$  gives the better result in the conventional molecular field model and therefore requires a weaker correction for agreement with the experimental data.

### 4. Nature of the activation energy $\Delta$

As one can see from Sec. 7, this simple model (it will be referred to below as the  $\Delta m\tau$  model) gives a temperature dependence of the electrical resistivity of the given oxide quite close to the experimental one. Here, however, a detailed microscopic picture of the phenomenon (i.e., mainly the nature of the activation energy  $\Delta$ ) is not considered. Moreover, we do not discuss here the values of all the fitting parameters (they are physically quite reasonable) and their exact origin. Obviously, behavior of the conductivity similar to that in the  $\Delta m\tau$  model can be obtained in a different way, but we suppose that this model is the simplest which takes into account the most important factors that can influence the magnetoresistive effect in doped manganites.

The activation energy  $\Delta$  in the model can reflect an effect of localization of the charge carriers [22] when the magnitude of the fluctuations of their exchange energies exceeds some critical value, at least for the majority of them at  $T \geq T_C$ . Apparently, a starting point for constructing a model of conductivity in manganites can be the concept of double exchange [23–25]. In reality the picture of the phenomenon appears to be more complex. The role of the charge carriers be played by magnetic polarons, which are being formed due to the interactions between the quasilocal charge carriers and magnetic

moments of the surrounding lattice sites, and due to deformations of the atomic structure over distances of the order of the first coordination sphere (see the general discussion in Refs. 22, 26, and 27 and the manganite-specific one in Refs. 2, 6, and 28). Note that the origin of the local lattice deformations can be of an exchange-relativistic nature [29]. There is no necessity, however, to make more precise the character of the charge carriers in the original  $\Delta m\tau$  model.

### 5. Experimental

The  $\text{La}_{1-x}\text{Ca}_x\text{MnO}_3$  ( $x \approx 1/3$ ) film (about 1500 Å thick) was grown by pulsed laser deposition on a  $\text{LaAlO}_3$  substrate. A KrF excimer laser operating at 248 nm was used to ablate the target material, with a nominal composition  $\text{La}_{2/3}\text{Ca}_{1/3}\text{MnO}_3$ . The target was prepared by the conventional solid-state reaction method starting from high-purity powders of  $\text{La}_2\text{O}_3$ ,  $\text{CaCO}_3$ , and  $\text{MnCO}_3$ . An x-ray study of the target has shown that it is homogeneous in composition and does not contain a residue of the starting chemical components. The film obtained was tested by the x-ray diffraction method and on an atomic force microscope. The resistance as a function of temperature (in the range 5–320 K) and magnetic field (up to 50 kOe) was measured by a standard four-point probe technique. The magneto-resistance  $\Xi(T, H) = [\rho(T, H) - \rho(T, 0)]/\rho(T, 0)$  was measured in a transverse geometry (with the field perpendicular to the film plane). The magnetization was measured by a SQUID magnetometer in the field range  $10 \text{ Oe} \leq H \leq 400 \text{ Oe}$  in a longitudinal geometry (with the field parallel to the film plane).

### 6. Results of experiment

Figures 1–7 present the following characteristics obtained for the  $\text{La}_{2/3}\text{Ca}_{1/3}\text{MnO}_3$  film studied: the square of the reduced magnetization  $(M(T)/M(0))^2$  in the Curie-point region, the reduced magnetization  $M(T)/M(0)$  at magnetic field  $H = 10 \text{ Oe}$ , the magnetization  $M(H)$  at temperatures of 10, 20, 40, and 60 K, the electrical resistivity  $\rho(T)$ , the electrical resistivity in a logarithmic scale, the logarithmic temperature derivative of the resistivity  $\partial \ln \rho / \partial T$ , and the magneto-resistance  $\Xi(T, H)$  in magnetic field  $H = 50 \text{ kOe}$ .

An extrapolation to  $\sigma = 0$  of the linear part of the dependence  $\sigma^2(T)$  (Fig. 1) gave a value of  $T_C$  equal to 267 K. The sharp growth of the magnetization below  $T_C$  seen in Fig. 2 confirms the high homogeneity of the film. The magnetic field depen-

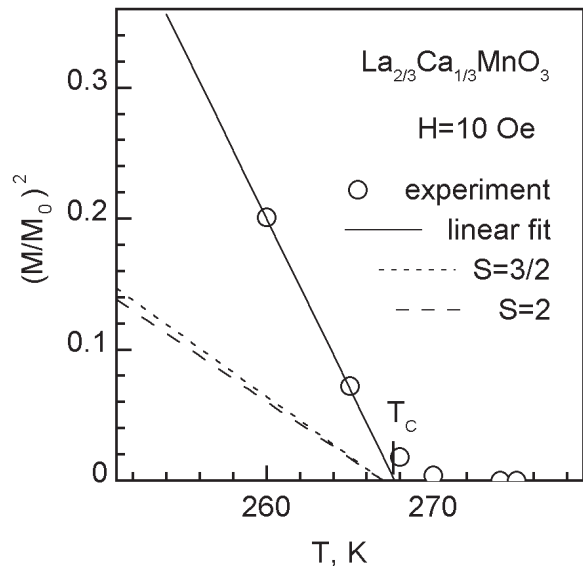


Fig. 1. Square of the reduced magnetization  $(M(T)/M(0))^2$  of the  $\text{La}_{2/3}\text{Ca}_{1/3}\text{MnO}_3$  film in a magnetic field  $H = 10 \text{ Oe}$  in the Curie-point region ( $\bullet$ ); the solid line determines the Curie point  $T_C$ ; the dashed and dotted lines show the expected dependences in the conventional molecular field model for spins  $S = 2$  and  $S = 3/2$ , respectively.

dence of the magnetization is found to be nonlinear in the temperature and magnetic field ranges studied (Fig. 3). At  $T = 10 \text{ K}$  the magnetization  $M$  is

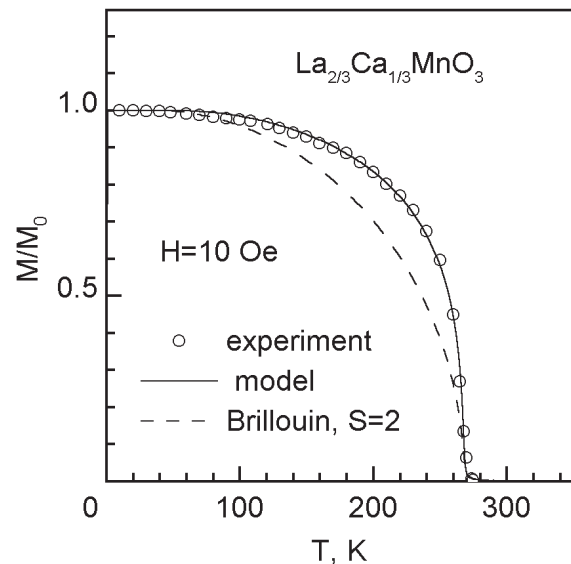


Fig. 2. Temperature dependence of the reduced magnetization  $M(T)/M(0)$  of the  $\text{La}_{2/3}\text{Ca}_{1/3}\text{MnO}_3$  film in a magnetic field  $H = 10 \text{ Oe}$  applied in the film surface plane: experiment ( $\bullet$ ) and calculations (solid line) in the modified molecular field model; the dashed line shows the  $M(T)/M(0)$  dependence in the conventional molecular field model (the Brillouin curve) for spin  $S = 2$ .

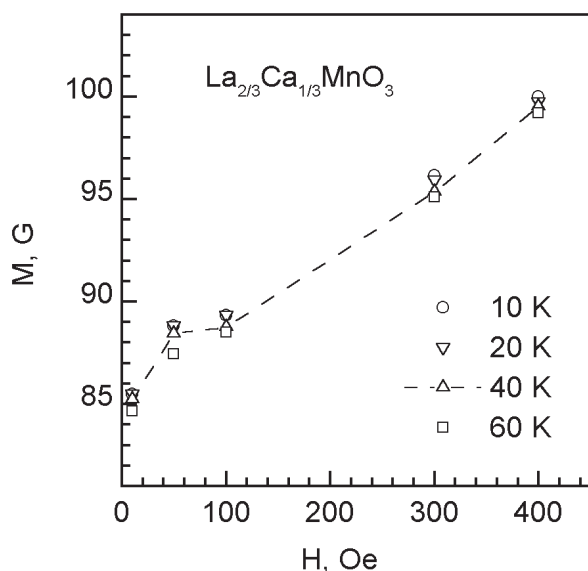


Fig. 3. Magnetization  $M(H)$  vs magnetic field  $H$  applied in the surface plane of the  $\text{La}_{2/3}\text{Ca}_{1/3}\text{MnO}_3$  film at temperatures of 10 K ( $\bullet$ ), 20 K ( $\nabla$ ), 40 K ( $\Delta$ ), and 60 K ( $\square$ ).

equal to 86 G at  $H = 10$  Oe, and it obeys the equation  $M[\text{G}] = 85 + 3.75 \cdot 10^{-2} H [\text{Oe}]$  in the range 100–400 Oe. The magnetic moment per Mn atom is equal to  $0.61 \mu_B$  at  $H = 400$  Oe. This shows that the magnetization is far from saturation in the field range under study.

As one can see from Fig. 4, the  $\rho(T)$  behavior has a semiconductive character above  $T_C$ . Below  $T_C$  the resistivity decreases sharply, falling to

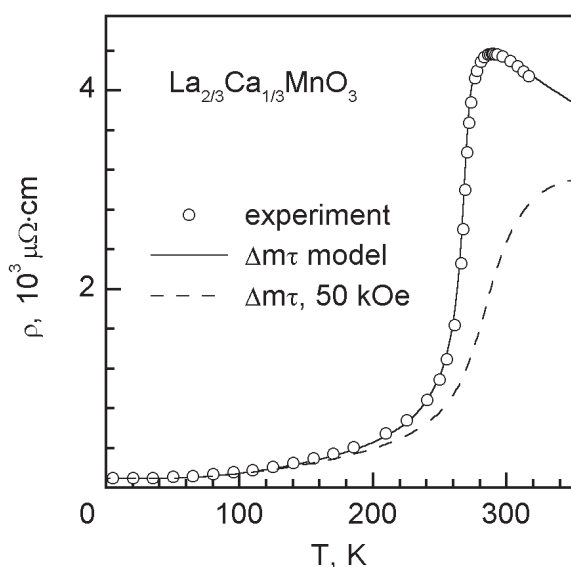


Fig. 4. Electrical resistivity of the  $\text{La}_{2/3}\text{Ca}_{1/3}\text{MnO}_3$  film vs temperature ( $\bullet$ ); the solid and dashed lines represent calculations in the  $\Delta m\tau$  model for magnetic fields of 0 and 50 kOe, respectively.

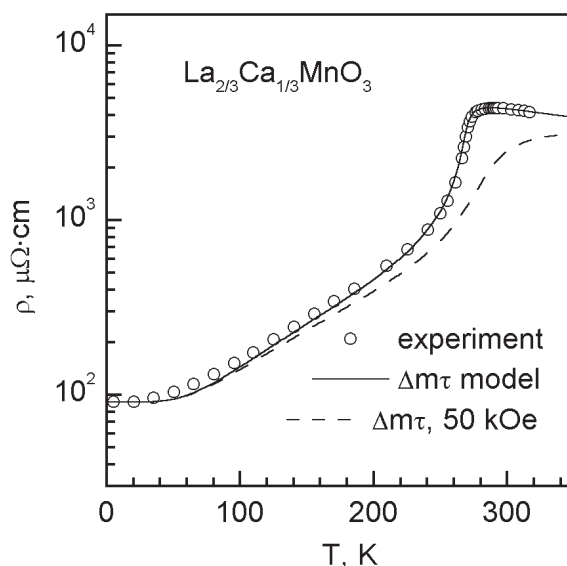


Fig. 5. Electrical resistivity of the  $\text{La}_{2/3}\text{Ca}_{1/3}\text{MnO}_3$  film vs temperature in logarithmic scale ( $\bullet$ ); the solid and dashed lines represent calculations in the  $\Delta m\tau$  model for magnetic fields of 0 and 50 kOe, respectively.

$\rho = 90.6 \mu\Omega \cdot \text{cm}$  at  $T = 5$  K. As is evident from Fig. 5, the dependence  $\rho(T)$  in a logarithmic scale (i.e.,  $\lg \rho(T)$ ) is close to linear in the range  $80 \text{ K} \leq T \leq 200 \text{ K}$ . The nearly constant value of the logarithmic derivative of  $\rho(T)$  seen in Fig. 6 also confirms the exponential temperature dependence of  $\rho(T)$  in this temperature range.

The temperature dependence of the  $\Xi$  at  $H = 50$  kOe presented in Fig. 7 is of the usual type

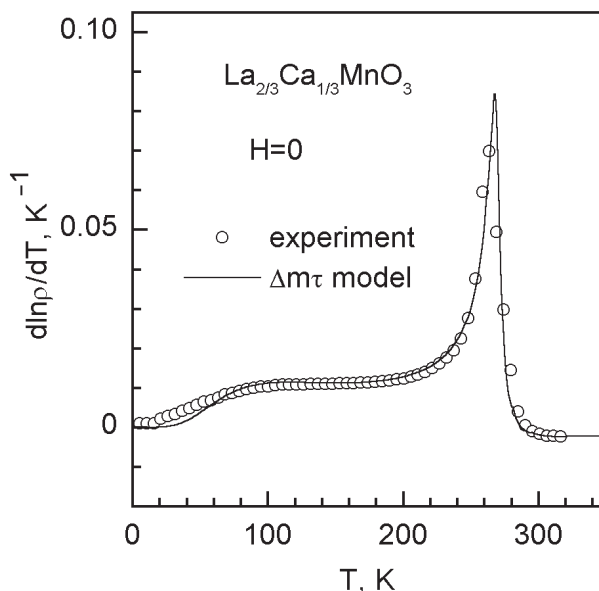


Fig. 6. The logarithmic temperature derivative of the electrical resistivity of the  $\text{La}_{2/3}\text{Ca}_{1/3}\text{MnO}_3$  film vs temperature ( $\bullet$ ); solid line represents the  $\Delta m\tau$  model calculations.

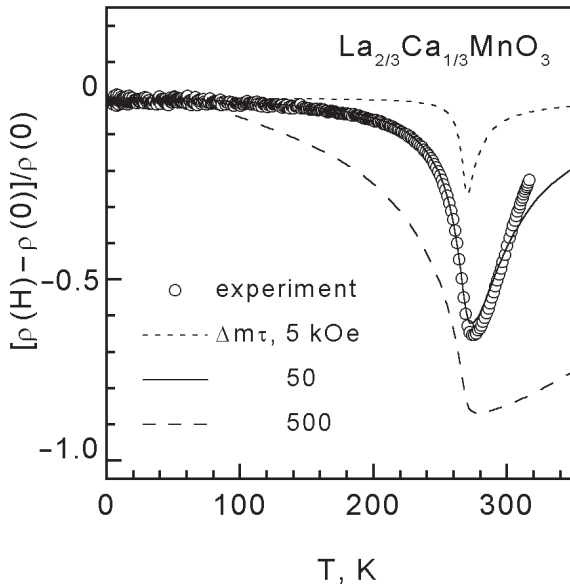


Fig. 7. Magnetoresistance  $[\rho(H) - \rho(0)]/\rho(0)$  of the  $\text{La}_{2/3}\text{Ca}_{1/3}\text{MnO}_3$  film vs temperature in a magnetic field of 50 kOe ( $\bullet$ ); the dotted, solid, and dashed lines represent the  $\Delta m\tau$  model calculations for magnetic fields of 5, 50, and 500 kOe, respectively.

for CMR manganites of fairly good crystal quality. It should be noted here that at the field 5 kOe the  $\Xi$  value was positive practically in the whole temperature range studied.

### 7. Comparison of the model and experimental data

The magnetization of the film, as one can see from Figs. 1 and 2, is substantially higher than that predicted by the conventional molecular field model ( $h = 0$ ,  $a = 0$  in Eq. (10)): the coefficient  $b$  in the formula  $\sigma^2 = b(1 - T/T_C)$ , which is valid in some neighborhood just below the Curie temperature, turned out to be about three times larger than the theoretical value (see Fig. 1). Possible reasons for this are a peculiarity of the double exchange [7] and an enhancement of the effective interatomic exchange interaction by the magnetoelastic coupling. The last has been taken into account in the modified molecular field model by the factor  $(1 - a\sigma^2)$  (in accordance with Ref. 21), which gives practically complete coincidence with the experimental data just below  $T_C$  (Fig. 2), in contrast to the results of Ref. 7, where the model curve increases faster than the experimental curve on lowering of the temperature.

Using Eqs. (1)–(10) and the experimental data on the magnetization and electrical resistivity, we obtained the following model parameters giving the best fit to the experimental data on resistivity pre-

sented in Fig. 4:  $\Delta_0 = 555$  K,  $\rho_0 = 90.6 \mu\Omega\cdot\text{cm}$ ,  $\rho_D = 400 \mu\Omega\cdot\text{cm}$ ,  $\rho_{mco} = 29.7 \mu\Omega\cdot\text{cm}$ ,  $h = 1$  K (this corresponds to a fictitious «short-range-order field» of about 3725 Oe),  $a = 0.26$ . The model temperature dependence  $\rho_{\text{mod}}(T)$  calculated with these parameters practically coincides with the experimental data for  $\rho(T)$  (see Fig. 4). The model temperature dependences  $\lg \rho_{\text{mod}}(T)$  and  $\partial \ln \rho_{\text{mod}}/\partial T$  also agree well with the experiment in the main temperature region (see Figs. 5, 6).

The numerical analysis has shown that the nearly linear in  $T$  region of the  $\lg \rho(T)$  dependence, which can be seen clearly (Fig. 5) in the range  $80 \text{ K} < T < 200 \text{ K}$ , as well as the nearly constant value of the  $\partial \ln \rho/\partial T$  derivative in the same temperature interval (see Fig. 6), are caused by the compensation of the bending «up» of the  $\Delta/T$  curve in the Eq. (6) by the bending «down» of the curve  $\lg [\rho_{\text{st}}(T) + \rho_{\text{ph}}(T) + \rho_m(T)]$ . The first can be seen from the approximation

$$\sigma(T) = g - pT - qT^2 - rT^3 - \dots,$$

where  $g$ ,  $p$ ,  $q$  and  $r$  are constants, which gives immediately the bending «up» curve:

$$\begin{aligned} \Delta/T &= \Delta_0 [1 - \sigma(T)]/T = \\ &= \Delta_0 [-(g - 1)/T + p + qT + rT^2 + \dots]. \end{aligned}$$

The second is caused by the  $\rho_{\text{ph}}(T)$  contribution (the contribution from  $\rho_m(T)$  is small in the temperature range under consideration, and the  $\rho_{\text{st}}$  value changes weakly there).

The character of the temperature dependence of the model magnetoresistive effect  $\Xi_{\text{mod}}(T, H) = [\rho_{\text{mod}}(h, T, H) - \rho_{\text{mod}}(h, T, 0)]/\rho_{\text{mod}}(h, T, 0)$  also corresponds rather well to the experiment at high magnetic fields (Fig. 7), though the accuracy in this case is somewhat lower: the maximal value at  $H = 50$  kOe is  $-0.65$  at  $T = 274$  K in the experiment, whereas the model gives  $-0.63$  at 273 K.

A somewhat unexpected finding is the experimental observation of a positive magnetoresistive effect with a maximum near  $T_C$  at low fields ( $H = 5$  kOe). In the framework of the  $\Delta m\tau$  model this can imply an increase of the activation energy  $\Delta$  and an enhancement of the electron scattering. One of the possible reasons may be the presence of an antiferromagnetic component in the magnetic structure of the system at low fields (see Refs. 14, 27, 30). In this case an increase of magnetization under the influence of the magnetic field should be accompanied by a reduction of the order parameter of the antiferromagnetic component and by a corresponding increase in the activation energy and electron scattering.

A detailed discussion of this effect is beyond the scope of this paper. In general, however, the character of the behavior of the model magnetoresistive effect  $\Xi_{\text{mod}}(H)$  in the interval  $0 < H < 75$  kOe at  $T = 273$  K is quite consistent with the experiment.

### 8. Conclusion

1. The magnetization  $M(T)$  and the electrical resistivity  $\rho(T)$  of a 150-nm thick  $\text{La}_{2/3}\text{Ca}_{1/3}\text{MnO}_3$  film have been studied in the temperature range  $5 \text{ K} \leq T \leq 320 \text{ K}$  in the magnetic field intervals  $10 \text{ Oe} \leq H \leq 400 \text{ Oe}$  and  $0 \leq H \leq 50 \text{ kOe}$ , respectively. It is found, that the  $M(T)/M(0)$  value is larger than that predicted by the conventional molecular field model below the Curie point  $T_C = 267 \text{ K}$ , and that the  $\lg \rho(T)$  dependence is close to linear ( $\lg \rho(T) = A + BT$ ) in the temperature range  $80 \text{ K} < T < 200 \text{ K}$  (accordingly  $\partial \ln \rho / \partial T$  is constant in this region).

2. A model of the electrical conductivity and magnetoresistivity of the system describing qualitatively the experimental results is proposed (the  $\Delta m \tau$  model). The model includes a thermally activated (with characteristic energy  $\Delta$ ) mechanism of conductivity, dependence of the concentration and the effective mass ( $m$ ) of the itinerant charge carriers on the magnetization, as well as scattering (with character time  $\tau$ ) of the charge carriers by static breakings of the translational symmetry, thermal fluctuations of the magnetic order, and phonons.

### Acknowledgment

Authors are pleased to dedicate the paper to Academician V. V. Eremenko, whose multifaceted scientific interests and achievements in the physics of magnetic phenomena in the compounds of  $d$  and  $f$  elements are widely appreciated.

1. E. L. Nagaev, *Phys. Usp.* **39**, 781 (1996).
2. J. M. D. Coey, M. Viret, and S. von Molnar, *Adv. Phys.* **48**, 167 (1999).
3. N. Furukawa, in: *Physics of Manganites*, T. A. Kaplan and S.D. Mahanti (eds.), Kluwer Academic, New York (1999), p.1.
4. V. M. Loktev and Yu. G. Pogorelov, *Fiz. Nizk. Temp.* **26**, 231 (2000) [*Low Temp. Phys.* **26**, 171 (2000)].
5. E. Dagotto, T. Hotta, and A. Moreo, *Phys. Rep.* **344**, 1 (2001).
6. M. Salamon and M. Jaime, *Rev. Mod. Phys.* **73**, 583 (2001).
7. C. W. Searle and S. T. Wang, *Can. J. Phys.* **48**, 2023 (1970).
8. T. Penney, M. W. Shafer, and J. B. Torrance, *Phys. Rev.* **B5**, 3669 (1972).
9. M. F. Hundley, M. Hawley, R. H. Heffner, Q. X. Jia, J. J. Neumeier, J. Tesmer, J. D. Thompson, and X. D. Wu, *Appl. Phys. Lett.* **67**, 860 (1995).
10. J. Z. Sun, L. Krusin-Elbaum, S. S. Parkin, and G. Xiao, *Appl. Phys. Lett.* **67**, 2726 (1995).
11. I. Esaki, P. J. Stiles, and S. von Molnar, *Phys. Rev. Lett.* **19**, 852 (1967).
12. N. Furukawa, *J. Phys. Soc. Jpn.* **64**, 3164 (1995).
13. M. Viret, L. Ranno, and J. M. D. Coey, *Phys. Rev.* **B55**, 8067 (1997-I).
14. J. Inoue and S. Maekawa, *Phys. Rev. Lett.* **74**, 3407 (1995).
15. A. J. Dekker, *J. Appl. Phys.* **36**, 906 (1965).
16. F. J. Blatt, *Physics of Electronic Conduction in Solids*, McGraw-Hill Book Company (1968).
17. T. Kasuya, *Progr. Theor. Phys.* **16**, 58 (1956).
18. H. Fujishiro, T. Fukase, M. Ikebe, and T. Kikuchi, *J. Phys. Soc. Jpn.* **68**, 1469 (1999).
19. M. R. Ibarra, P. A. Algarabel, C. Marquina, J. Blasco, and J. Garcia, *Phys. Rev. Lett.* **75**, 3541 (1995).
20. S. V. Vonsovsky, *Magnetism*, Wiley, New York (1974).
21. A.B. Beznosov, E. L. Fertman, V. V. Eremenko, P. P. Pal-Val, V. P. Popov, and N. N. Chebotayev, *Fiz. Nizk. Temp.* **27**, 430 (2001) [*Low Temp. Phys.* **27**, 320 (2001)].
22. N. F. Mott and E. A. Devis, *Electron Processes in Non-Crystalline Materials*, Clarendon Press, Oxford (1979).
23. C. Zener, *Phys. Rev.* **82**, 440 (1951).
24. P. W. Anderson and H. Hasegawa, *Phys. Rev.* **100**, 675 (1955).
25. P.-G. de Gennes, *Phys. Rev.* **118**, 141 (1960).
26. S. Methfessel and D. C. Mattis, *Magnetic Semiconductors*, Springer-Verlag, New York (1968).
27. E. L. Nagaev, *Physics of Magnetic Semiconductors*, Mir, Moscow (1983).
28. J. M. De Teresa, M. R. Ibarra, P. A. Algarabel, C. Ritter, C. Marquina, J. Blasco, J. Garcia, A. del Moral, and Z. Arnold, *Nature* **386**, 256 (1997).
29. V. V. Eremenko, A. B. Beznosov, E. L. Fertman, P. P. Pal-Val, and V. P. Popov, *Adv. Cryogenic Eng.* **46**, 413 (2000).
30. J. Jiang, J. Dong, and D. Y. Xing, *Phys. Rev.* **B55**, 8973 (1997-II).